— Article —

The Effect of Platinum Deposition on the Water Photo-Reduction at p-Cu_2O Semiconductor Electrodes with Visible Light Irradiation

Ponchio CHATCHAI,[a,b] Atsuko Y. NOSAKA,[a] and Yoshio NOSAKA[a,*]

[a]Department of Materials Science and Technology, Nagaoka University of Technology, (1603-1 Kamitomioka, Nagaoka, Niigata 940-2188 Japan)
[b]Department of Chemistry, Faculty of Science and Technology Rajamangala University of Technology (Klong 6 Thanyaburi Pathumthani, 12110 Thailand)

Received April 2, 2011 ; Accepted May 24, 2011

The surface of a p-Cu_2O semiconductor photoelectrode was modified by electrodeposition of Pt nanoparticles and analyzed by XRD, SEM, XPS, and EIS (electrochemical impedance spectrometry) methods besides photocurrent measurements. The XRD, SEM, and XPS analyses showed the fabrication of Cu_2O film and the deposition of Pt particles. On the electrodeposition of Pt nanoparticles, cathodic photocurrent was enhanced. The EIS analysis suggested that Pt nanoparticles enhance the charge transfer process to the solution.

Key Words : Cu_2O Photoelectrode, Pt Nanoparticles, Hydrogen Evolution, Photoelectrocatalysis,

1 Introduction

Photoelectrochemical water splitting driven by solar light energy is one of the attractive targets for the development of hydrogen fuel production systems, because it is an ultimate solution for solving both the energy and environmental problems. Many metal oxide semiconductors working in a visible light region have been developed as photoelectrodes for water splitting.[1-5] Recently, we have reported $BiVO_4$ electrodes coupled with SnO_2 and WO_3 thin layers[6-7] in order to develop a photo-anode with a high activity of oxygen evolution under visible light irradiation. Moreover, gold nanoparticles were deposited on WO_3/$BiVO_4$ photoelectrode and the anodic photocurrent was increased.[8] Since these electrodes are n-type semiconductors and the potential is not enough for water reduction, p-type semiconductors have been expected as a photo-cathode for water reduction. As an efficient photo-cathode was prepared, a tandem-type photoelectrochemical cell[9] for solar water splitting can be fabricated with the photo-anode reported.

A p-type copper (I) oxide (Cu_2O) semiconductor is one of the most attractive materials because the band gap energy is so narrow (2.0-2.2 eV) enough to absorb efficiently the solar light, and the conduction band level is negative enough for the reduction of water.[10,11] Various researchers on the photocatalytic properties of Cu_2O have been reported. Hara *et al.*[12] investigated the photocatalytic water spitting to H_2 and O_2 on Cu_2O powder. However, the mechanism of the process was not clear. To clarify the mechanism, Jongh *et al.*[13] studied the electrochemical photocatalytic properties of Cu_2O electrode of water decomposition. They concluded that the Cu_2O band gap energy is suitable to reduce water to hydrogen than that the water oxidation as consider in the level of energy bands. Although p-Cu_2O is used as a photo-cathode towards hydrogen evolution under visible light irradiation, the photocatalytic activity of pure Cu_2O is unusually low because of the recombination of the photogenerated electrons and holes. This effect was studied by Nagasubramanian *et al.*[14] who confirmed the rapid recombination processes of p-Cu_2O in acetonitrile solution. There are many reports on preventing the recombination to enhance charge separation in Cu_2O semiconductor. The charge separation could be improved by trapping electrons at the conduction band of Cu_2O.[15] It may possible to improve the charge separation by combining an n-type WO_3 with the p-type Cu_2O electrode for H_2 evolution.[16] Assembling of metal nanoparticles on the semiconductor surface is one of the strategies to achieve a high catalytic activity. We found in the previous study that the modification with gold nanoparticles could improve the surface properties of a $BiVO_4$ electrode to enhance the water oxidation.[8] Therefore, metal nanoparticles were expected to modify the Cu_2O surface to promote the photocatalytic activity for water reduction.

Platinum is an attractive metal because of the high catalytic activity with a low over potential for hydrogen evolution.[17,18] Peruffo *et al.* reported an electrochemical method which enabled direct deposition of Pt nanoparticles on a fluorine-doped thin oxide (FTO) substrate, exhibiting an enhanced electrocatalytic activity.[19] Therefore, in the present study we examined the electrodeposition of Pt nanoparticles on an FTO/Cu_2O electrode and evaluated their photocatalytic activities for hydrogen evolution under visible light irradiation.

2 Experimental

2.1 Preparation of the FTO/Cu_2O film photoelectrode

Cu_2O thin films were fabricated on a conducting FTO substrate by electrodeposition. The electrolyte was consisted of 0.1 M (M = mol dm^{-3}) of $CuSO_4$ and 0.1 M of tartaric acid,[20] and the pH was adjusted to 9.0 with 3.0 M

NaOH. The constant potential of −0.4 V was applied to the FTO substrate using a three electrode system with a platinum coil counter electrode and an Ag/AgCl (3.0M KCl) reference electrode (BAS Inc., RE-7). The temperature of the solution was kept at 80℃ during electro-deposition. The deposited Cu_2O film was dried at 150℃ for 60 min and then the edges of the photo-electrodes were covered with epoxy resin to confine the irradiation area to be 1 cm^2. The deposition time for Cu_2O was selected to be 7 min, because the resultant electrode showed a highest cathodic photocurrent.

2.2 The modification of FTO/Cu_2O electrodes with Pt nanoparticles

Pt nanoparticles were deposited on the Cu_2O electrode by the electrodeposition using an aqueous solution of 5 mM K_2PtCl_6 under N_2-saturated condition.[21] After the deposition, the modified electrode was dried at 150℃ for 60 min. The deposition of Pt on Cu_2O electrode was checked by measuring cyclic voltammograms at −0.7 to 0.5 V in 0.5 M Na_2SO_4 solution under dark condition, where Pt oxidation and the corresponding reduction currents were observed. The condition of electrodeposition which provides the maximum photocurrent was the deposition potential of −0.5 V (vs. Ag^+/AgCl) and the deposition time of 8 min. Under this condition the FTO/Cu_2O/Pt electrodes used in the present study were prepared.

2.3 Photoelectrochemical measurement and characterization

The optical absorption spectra of the composite electrodes were measured by using a UV/Vis spectrophotometer (Shimadzu, UV-3150). The morphology of the electrodes was examined by using a scanning electron microscope (SEM), (Technex Co., Tiny-SEM 1710) . X-ray photoelectron spectroscopy (XPS) measurements were carried out using a JPS-9010TR (JEOL) spectrometer equipped with a monochromatic Mg Kα source. X-ray diffraction (XRD) patterns were recorded with a M03HF22 diffract meter (MAC Science, Inc.) using Cu Kα radiation.

Photocurrent was measured in a N_2-saturated aqueous solution of 0.5 M Na_2SO_4 by a three-electrode system with a Pt coil counter electrode and the Ag/AgCl reference electrode. A voltammetry analyzer (Princeton Applied Research, Versa STAT^3) was used in the modes of cyclic voltammetry and linear scan voltammetry. For photo-irradiation, a 50-W tungsten lamp (Moritex, MHF-C50LR) was used. A 420-nm sharp-cut glass filter (HOYA, L-42) was inserted across the light path to confine the wavelength of light to visible region. The electrochemical impedance spectrometry (EIS) was performed with the voltammetry analyzer under the applied potential of −0.5 V (vs. Ag/AgCl) at frequencies ranging from 100 kHz to 0.1 Hz under irradiation of the visible light.

3 Results and Discussion

3.1 Characterization of the film electrodes

The FTO/Cu_2O film photoelectrode shows a brick red color that corresponds to that of cuprous oxide (Cu_2O).[22] Figure 1 shows the absorption spectra of the FTO/Cu_2O and other electrodes. The absorption edge for FTO/Cu_2O and FTO/Cu_2O/Pt was around 650 nm. This absorption edge reasonably agrees with the reported band-gap energy of Cu_2O semiconductor (2.0-2.2 eV).[11,23] The FTO/Cu_2O/Pt electrode shows a similar absorption spectrum to that of the FTO/Cu_2O electrode, indicating that the main absorption properties of the Pt-deposited electrode originate from a Cu_2O semiconductor. The increase in the absorbance of the FTO/Cu_2O/Pt electrodes is attributable to the scattering effect of the Pt nanoparticle layer, because the FTO/Pt electrode (Spectrum C) shows the higher absorbance than that of the FTO electrode (D) where no absorption peak was observed in the whole wavelength region.

Figure 2 shows a top view (left side) and a cross-sectional view (right side) of SEM images for (A) FTO substrate, (B) FTO/Cu_2O, and (C) FTO/Cu_2O/Pt electrodes. As shown in Fig. 2 (B), the morphology of FTO/Cu_2O was pyramid shape, which corresponds to the (111) crystallographic plane of Cu_2O.[10] The (111) crystalline surface was reported to contribute to a high photocatalytic activity for H_2-evolution.[16] In the cross sectional view (right) the boundary between FTO and Cu_2O was not clearly observed. Since the thicknesses of the FTO and FTO/Cu_2O layers were 1.8 μm and 3.4 μm, respectively, the thickness of the Cu_2O layer is estimated to be about 1.6 μm. For FTO/Cu_2O/Pt electrodes (Fig. 2 (C)), though the Pt layer could not be distinguished from the cross-sectional view, from the top view the pyramidal Cu_2O crystallites was suspected to be covered by the Pt particles deposited on the surface.

The crystalline phase of film photoelectrodes was confirmed by XRD measurements. The XRD pattern of the FTO/Cu_2O electrode shows a distinct cubic Cu_2O crystal

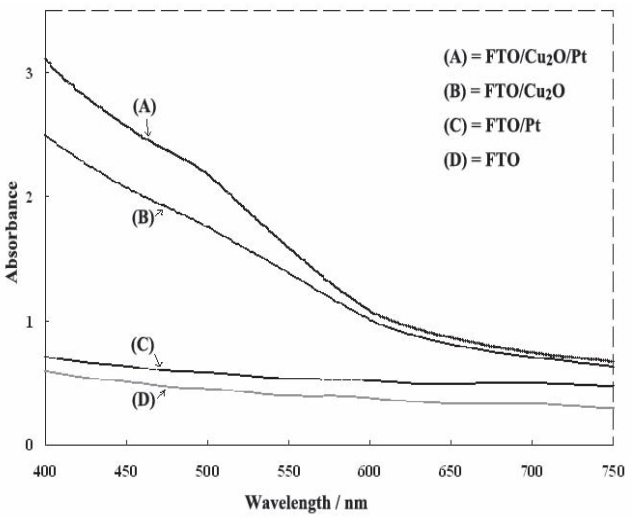

Fig. 1 UV/Vis absorption spectra of (A) FTO/Cu_2O/Pt, (B) FTO/Cu_2O, (C) FTO/Pt, and (D) FTO electrodes.

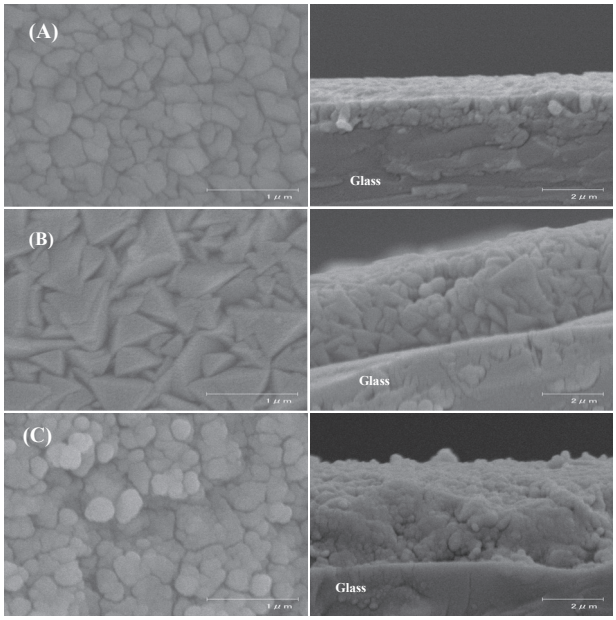

Fig. 2 Scanning electron micrograph (SEM) images of (A) FTO, (B) FTO/Cu_2O, and (C) FTO/Cu_2O/Pt electrodes. The left panels represent the top view and the right panels represent the cross-sectional view.

with 2θ of 36.5°, 42.4° and 61.5°, which correspond to (111), (200) and (220) planes,[10,24] respectively. For FTO/Cu_2O/Pt electrode, no diffraction peak of Pt was observed by XRD measurements in the present study, because the amount of Pt particles was too small.

The presence and the oxidation state of Cu and Pt were evaluated by XPS measurements. Figure 3 (A) shows the XPS peaks of $Cu2p_{3/2}$ and $Cu2p_{1/2}$ observed for FTO/Cu_2O/Pt electrode before and after Ar^+ etching. The peaks at 933 and 953 eV are attributable to Cu_2O,[24,25] while the peaks at 943 and 963 eV are assigned to those of the CuO.[26] By the Ar^+ etching, the signal intensity increased due to the partial removal of Pt at the surface. The relative peak intensity for Cu_2O to CuO was increased after the Ar^+ etching, indicating that Cu^+ (in Cu_2O) changed to Cu^{2+} (in CuO) at the surface in the Pt-deposition process. Figure 3 (B) shows the Pt4f peaks in the XPS spectra. Before Ar^+ etching the peak positions of $Pt4f_{7/2}$ for FTO/Cu_2O/Pt (72.7eV) is distant from that of the metallic Pt, which was 71.1 eV FTO/Pt (not shown). The broad peaks for Pt4f signals appeared before Ar^+ ion etching consist of peaks at 72.7-76 eV for $4f_{7/2}$ and at 75-78 eV for $4f_{5/2}$. These are attributable to various oxidized Pt species at the surface, which species may be Pt hydroxides and dioxides since $4f_{7/2}$ peaks for $Pt(OH)_2$ and PtO_2 appear at 72.6-72.8 and 74.6-75.6 eV, respectively.[27] After Ar^+-etching the Pt4f peak position for the FTO/Cu_2O/Pt moved from 72.7 to 71.2 eV, indicating the oxidized Pt located only at the outermost surface. Thus these XPS results for the FTO/Cu_2O/Pt electrode clearly verify the formation of Pt metal on the Cu_2O layer.

3.2 Photoelectrochemical properties

Cyclic voltammograms were measured to study the oxidation and reduction properties of the FTO/Cu_2O and

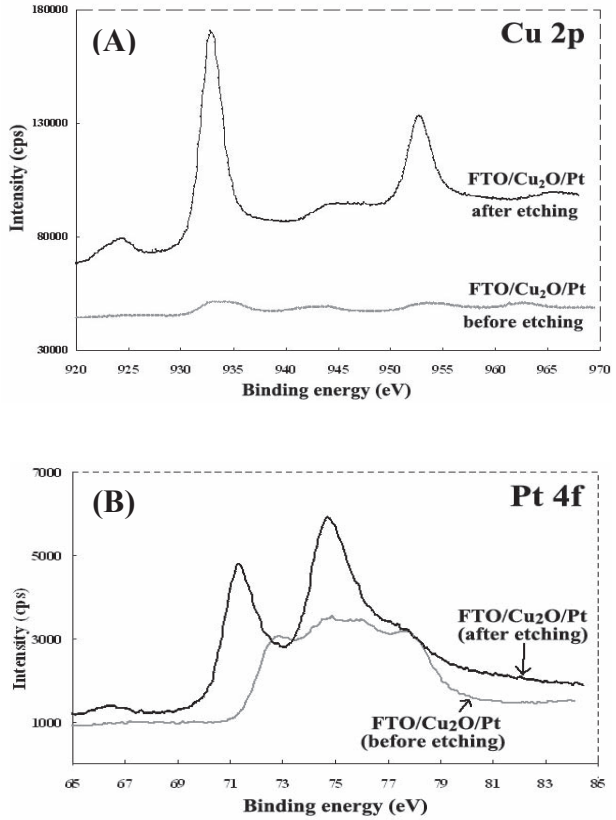

Fig. 3 The XPS spectra in (A) Cu2p and (B) Pt4f core level regions for FTO/Cu_2O/Pt electrode before and after Ar^+-etching The binding energy was calibrated by C 1s.

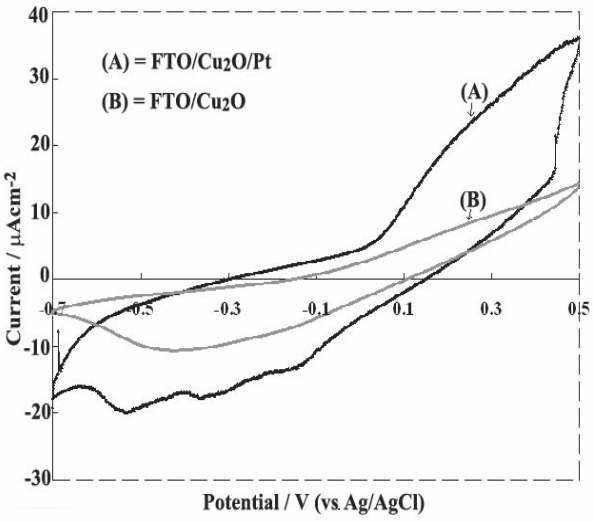

Fig. 4 Cyclic voltammograms comparing the FTO/Cu_2O with FTO/Cu_2O/Pt composite electrodes in 0.5 M Na_2SO_4 aqueous solution under the dark condition. Scan rate was 50 mV s^{-1}. Electrolyte solution was deaerated by N_2 gas.

FTO/Cu_2O/Pt electrodes under the dark condition in saturated N_2 solution of Na_2SO_4 (Fig. 4). The FTO/Cu_2O/Pt electrode showed two reduction peaks at around −0.35 and −0.55 V which are attributable to the reduction peaks of hydrogen adsorption at the Pt surface.[21] The oxidation and reduction peaks at 0.1 V and −0.1 V

vs. Ag/AgCl correspond to the oxidation of Pt metal to Pt oxide and the reduction of Pt oxide to Pt metal, respectively.[17,21]

Figure 5 shows the linear scan voltammograms in which the FTO/Cu_2O electrode was compared with the FTO/Cu_2O/Pt electrode under periodical visible light illumination. The onset of cathodic photocurrents around −0.25 V (vs. Ag/AgCl at pH = 6) is consistent with the conduction band bottom of p-type Cu_2O semiconductor.[11] For the both electrodes, cathodic photocurrent increased slowly with the application of more negative potential, indicating rather rapid carrier recombination. The FTO/Cu_2O/Pt electrode presents a significantly higher cathodic photocurrent than that of the FTO/Cu_2O electrode at the potentials ranging from −0.25 to −0.70 V. Thus, these results could confirm that the Pt nanoparticles promoted the electrocatalytic activity by the enhancement of the charge transfer process for water reduction process.

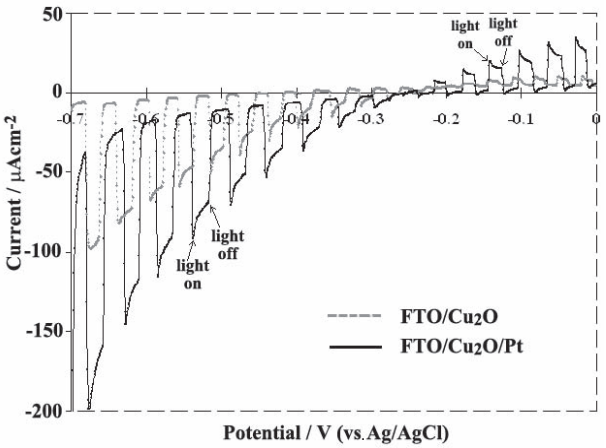

Fig. 5 Linear scan voltammograms for the FTO/Cu_2O and FTO/Cu_2O/Pt electrodes at the potentials ranging from −0.7 to 0.0 V vs. Ag/AgCl in N_2-bubled 0.5 M Na_2SO_4 aqueous solution under periodical visible light illuminations.

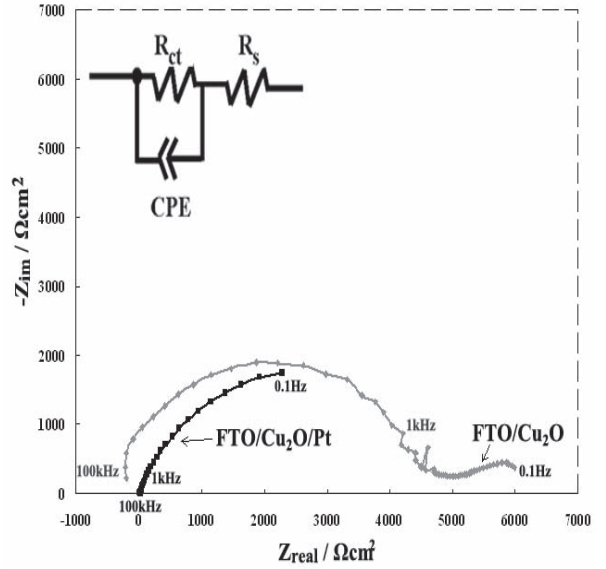

Fig. 6 Nyquist plots for the FTO/Cu_2O and FTO/Cu_2O/Pt electrodes in N_2-bubled 0.5 M Na_2SO_4 aqueous solution under visible light illuminations. The applied potential was −0.5 V vs. Ag/AgCl. The inset shows the equivalent circuit for the analysis.

Under anodic polarization, anodic photocurrent was observed with the visible light irradiation at a potential above −0.25 V especially for the Pt deposited electrode. This increase in the anodic photocurrent is attributable to the collapse of Schottky barrier by the formation of surface states and then the photocurrent at anodic polarization was allowed on the Pt deposition.

EIS measurements were performed to characterize an electrochemical interfacial reaction of FTO/Cu_2O/Pt electrode for water reduction under the visible light irradiation. Figure 6 shows Nyquist plots of FTO/Cu_2O and FTO/Cu_2O/Pt electrode in aqueous Na_2SO_4 solution under the applied potential of −0.5 V (vs. Ag/AgCl). The simple equivalent circuit (inset of Fig. 6) used consists of a solution resistance (R_s), charge transfer resistance (R_{ct}) and constant phase elements (CPE). The diameter of the semicircle usually equals to the R_{ct} parameter, which corresponds to the efficiency of the charge transfer at the electrode interface. The CPE is divided into two parameters, CPE-T and CPE-P, by using an analyzing program "Z-view" based on the equivalent circuit. The CPE-P is a parameter indicating the pure capacitor properties, while CPE-T represents the capacitance of CPE, which is applied often to analyze non-homogeneous systems. If CPE-P is unity, the CPE-T becomes identical to that of a capacitor.[28] The parallel combination of R_{ct} and CPE leads to characteristics of the semicircle in the Nyquist plot. The values of EIS parameters obtained by the analysis were shown in Table 1. Since the value of CPE-P is around 0.8 for both electrodes these electrodes almost act as nearly a capacitor, and then the CPE-T parameter can be treated as a capacitor. By comparing the simulated result, the R_{ct} value of FTO/Cu_2O/Pt was smaller than that of FTO/Cu_2O electrodes, suggesting that the electron transfer rate at FTO/Cu_2O/Pt is faster than that of FTO/Cu_2O electrode. The CPE-T value of FTO/Cu_2O/Pt shows significantly higher than that of the FTO/Cu_2O electrode. The significant increase in the capacitance by the modification with Pt nanoparticles may be partly explained by the increase of the surface roughness by Pt deposition on the Cu_2O surface as presented by SEM observation.

Table 1 Impedance components for water reduction on the FTO/Cu_2O and FTO/Cu_2O/Pt electrode determined by fitting the experimental data to the equivalent circuit shown in Fig. 6.

Photoelectrodes	R_{ct}/kΩcm^2	CPE-T/μFcm^{-2}	CPE-P
FTO/Cu_2O	5.02	0.03	0.83
FTO/Cu_2O/Pt	4.53	320	0.8

4 Conclusions

The modified Cu_2O with Pt nanoparticles was fabricated by a simple and quick electrodeposition technique. The fabrication of Cu_2O/Pt photoelectrodes could be confirmed by SEM, XRD and XPS measurements; as-deposited Cu_2O/Pt composite films are composed of pyramidal shape of cubic Cu_2O and nanoparticles of metallic Pt. The Pt nanoparticles on the surface of Cu_2O act as a catalyst for preventing the photogenerated electrons from the recombination. Especially, Pt of a small particle size could affect the roughness of electrode surface for efficient water reduction. Therefore, this modified electrode is suitable to the use as a photo-cathode and to be combined with a photo-anode for making a highly efficient water splitting cell for solar energy conversion.

Reference

1) K. Sayama, A. Nomura, T. Arai, and H. Sugihara, *J. Phys. Chem. B,* **110**, 11352 (2006).
2) A. Kudo, *Int. J. Hydrogen Energ.,* **32**, 2673 (2007).
3) A. Enesca, A. Duta, and J. Schoonman, *Thin Solid Films,* **515**, 6371 (2007).
4) C. Xu, Y. A. Shaban, and S. U. M. Khan, *Sol. Energ. Mater. Sol. Cell.,* **91**, 938 (2007).
5) H. Liu, R. Nakamura, and Y. Nakato, *Chem. Phys. Chem.,* **6**, 2499 (2005).
6) P. Chatchai, Y. Murakami, S. Kishioka, A. Y. Nosaka, and Y. Nosaka, *Electrochem. Solid-State Lett.,* **11**, H160 (2008).
7) P. Chatchai, Y. Murakami, S. Kishioka, A. Y. Nosaka, and Y. Nosaka, *Electrochim. Acta,* **54**, 147 (2009).
8) P. Chatchai, S. Kishioka, Y. Murakami, A. Y. Nosaka, and Y. Nosaka, *Electrochim. Acta,* **55**, 592 (2010).
9) M. Woodhouse and B. A. Parkinson, *Chem. Soc. Rev.,* **38**, 197 (2009).
10) L. C. Wang, N. R. de Tacconi, C. R. Chenthamarakshan, K. Rajeshwar, and M. Tao, *Thin Solid Films,* **515**, 3090 (2007).
11) S. Somasundaram, C. R. Chenthamarakshan, N. R. de Tacconi, and K. Rajeshwar, *Int. J. Hydrogen Energ.,* **32**, 4661 (2007).
12) M. Hara, T. Kondo, M. Komoda, S. Ikeda, K. Shinohara, A. Tanaka, J. N. Kondo, and K. Domen, *Chem. Commun.*, 357 (1998).
13) P. E. De Jongh, D. Vanmaekelbergh, and J. J. Kelly, *Chem. Commun.*, 1069 (1999).
14) G. Nagasubramanian, A. S. Bioda, and A. J. Bard, *J. Electrochem. Soc.,* **128**, 2158 (1981).
15) J. P. Yasomanee and J. Bandara, *Sol. Energ. Mater. Sol. Cell.,* **92**, 348 (2008).
16) C. C. Hu, J. N. Nian, and H. Teng, *Sol. Energ. Mater. Sol. Cell.,* **92**, 1071(2008).
17) X. Zhang, D. Dong, D. Li, T. Williams, H. Wang, and P. A. Webley, *Electrochem. Commun.,* **11**, 190 (2009).
18) T. Sasaki, N. Koshizaki, J. W. Yoon, and K. M. Beck, *J. Photochem. Photobiol. A,* **145**, 11 (2001).
19) M. Peruffo, P. C. Carballada, P. Bertoncello, R. M. Williams, L. D. Cola, and P. R. Unwin, *Electrochem. Commun.* **11**, 1885 (2009).
20) T. Fujiwara, T. Nakaue, and M. Yashimura, *Solid State Ionics,* **175**, 541 (2004).
21) H. B. Hassan, *J. Fuel Chem. Technol.,* **37**, 346 (2009).
22) T. Mahlingam, J. S. P. Chitra, J. P. Chu, S. Velumani, and P. J. Sebastian, *Sol. Energ. Mater. Sol. Cell.,* **88**, 209(2005).
23) Y. Bessekhouad, D. Robert, and J.-V. Weber, *Catal. Today,* **101**, 315 (2005).
24) K. P. Muthe, J. C. Vyas, and S. C. Sabharwal, *Thin Solid Films,* **324**, 37 (1998).
25) J. Morales, L. Sanchez, F. Martin, and M. Sanchez, *Electrochim. Acta,* **49**, 4589 (2004).
26) L. Huang, F. Peng, and F. S. Ohuchi, *Surf. Sci.,* **603**, 2825 (2009).
27) http://srdata.nist.gov/xps/
28) Y. Lin and X. Cui, *Langmuir,* **21**, 11474 (2005).